OL Organic Letters

Visible-Light-Triggered Iodinations Facilitated by Weak Electrostatic Interaction of N-Heterocyclic Carbenes

He Sheng, Qiang Liu, Xiao-Di Su, Yu Lu, Zhi-Xiang Wang,* and Xiang-Yu Chen*

Cite This: https://dx.doi.org/10.1021/acs.orglett.0c02523 **Read Online**

ABSTRACT: N-heterocyclic carbenes (NHCs) are well-known as ligands and organocatalysts, but there is no recognition for their catalytic role as a stabilizer through electrostatic interaction rather than electron donation. By utilizing the electrostatic interaction, we herein describe the success of a visible-light-triggered radical−radical cross-coupling of N-alkenoxypyridinium salts and NaI, giving a variety of α-iodo ketones. Computational studies characterize the stabilization role of NHCs.

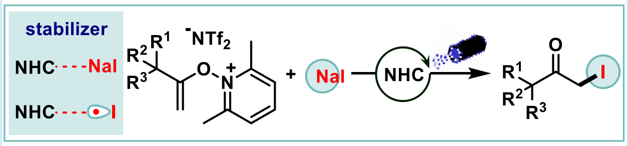

As ligands and organocatalysts, N-heterocyclic carbenes (NHCs) serve a prominent role in developing novel catalytic processes.[1] Recently, there has been emerging interest in harnessing the synergistic interplay of NHCs[2] and photochemistry[3] to discover new activation modes that offer more efficient and selective alternatives to orthodox approaches. In 2012, Rovis and co-workers first reported the photoredox/NHC dual-catalyzed α-acylation of tertiary amines with aldehydes.[4] Very recently, significant progress has been achieved in the field of cooperative NHC catalysis and light activation by the research groups of Sun,[5] Ye,[6] Hopkinson,[7] Scheidt,[8] and Studer.[9] All these strategies were based on the formation of NHC-derived intermediates,[10] which can directly react with partners under the excitation of light (Scheme 1A). As such, these approaches often require judiciously choosing the carbonyl compounds to generate the NHC-derived intermediates and the corresponding reaction partners, which could be an impediment to the reaction generality. Additionally, expensive metal-based photocatalysts or harmful UV-light were generally required for these transformations. In this context, the discovery of new applications of NHCs with the excitation of visible light which allows flexible and various substitution patterns is of great value and highly desirable.

The interaction between Lewis bases and alkali metal cations plays an important role in organic synthesis, catalysis, and medicinal chemistry.[11] In 2017, Krieck and Westerhausen and co-workers established that the electrostatic interaction of NHC and NaI enabled the construction of new architectures (Scheme 1B).[12] In this study, we drew inspiration from the photochemistry of an electron donor−acceptor (EDA) complex,[13] which serves as an alternative and complementary approach to photoredox catalysis to avoid using expensive metal complexes and organic dyes. As shown in Scheme 1C, we hypothesized that the NHC-stabilized NaI can form an EDA complex with an electron acceptor, which could be activated by visible light to undergo single electron transfer (SET), generating an alkyl radical and iodine radical. In addition, the generated iodine radical could be stabilized by the NHC,[14] which may benefit the subsequent radical−radical coupling.

Iodine compounds have versatile applications in various synthetically important bond formations, synthesis of drugs, contrastors, and radioactively labeled markers.[15] In 2015, Li and co-workers developed an elegant UV-light-induced approach to aryl iodides via the radical coupling of sodium iodide.[16] Recently, Fu and Shang reported a novel PPh$_3$/NaI mediated photocatalytic decarboxylative alkylation via PPh$_3$−I$^\bullet$ species, in which the cation−π interaction of PPh$_3$ and Na$^+$ was crucial for the EDA complex formation. Intriguingly, no iodination product was observed in their system.[17]

With this knowledge, a mixture of *N*-alkenoxypyridinium salt[18] and NaI in MeCN was irradiated with blue LEDs (λ = 455 nm) at room temperature. The iodination product **2** was obtained in 51% yield, while no reaction was observed in the absence of light (Scheme 2A), indicating the formation of an EDA complex between **1** and NaI. Encouraged by this promising result, we envisioned that our hypothesis could be devised to improve the efficiency of the iodinations, and we were pleased to find that the desired product **2** was obtained in 85% yield in the presence of precatalyst **A**. A catalyst screening showed that other precatalysts **B**−**D** and PPh$_3$ gave poorer yields. The reaction outcome was further improved to 92% yield by using LiNTf$_2$ as an ion exchange additive to increase the solubility of NHC salt (Scheme 2B). Unfortunately, further optimization of the catalyst loading (10 mol %) gave a decreased 65% yield. To understand this radical−radical

Received: July 29, 2020

Scheme 1. Motivation and Synthetic Strategy

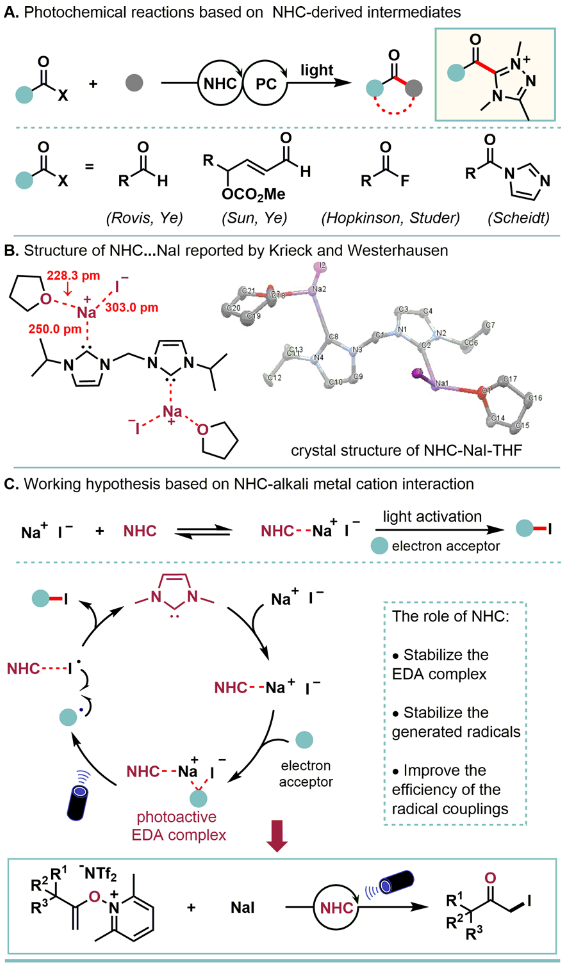

Scheme 2. Optimization of the Reaction Conditions

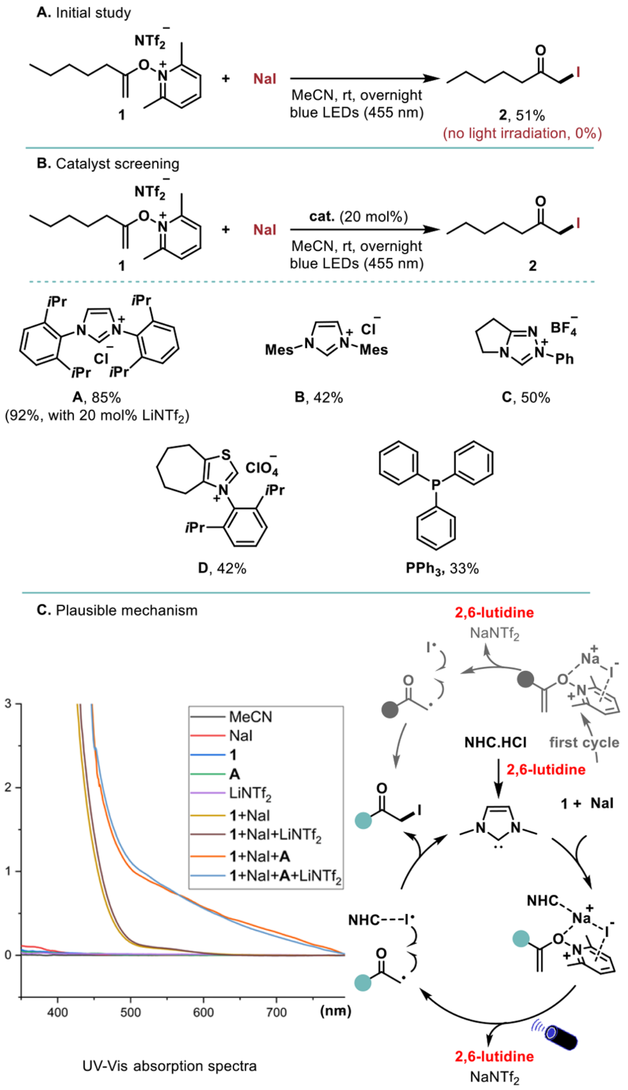

coupling process, we turned to characterize the EDA complex and the role of the NHC. While neither *N*-alkenoxypyridinium salt **1** nor NaI showed significant UV/vis absorption in the visible region of the spectra, an obvious red shift of absorption was observed in the spectrum of the reaction mixture **1** and NaI, supporting the formation of an EDA complex (Scheme 2C, left). The addition of NHC **A** further enhanced the red shift of absorption, thus facilitating the EDA complex formation. The plausible mechanism shown in Scheme 2C (right) would possibly explain the role of NHC. Irradiation of EDA complex of **1** and NaI generates the alkyl radical, iodine radical, and 2,6-lutidine. The following radical−radical coupling gives the iodination product. Concomitantly, the NHC is formed via deprotonation of the corresponding azolium salt by the in situ generation of 2,6-lutidine. The electrostatic interaction of NHC···NaI would facilitate the formation of the EDA complex. In addition, the 2c−3e interaction of NHC could stabilize the generated iodine radical, thus improving the efficiency of the iodinations.

With the optimized conditions in hand, we subsequently examined the generality of the method (Scheme 3). We successfully converted a range of unfunctional alkenoxypyridiniums into the corresponding *α*-iodo ketones, with acyclic and cyclic alkyl groups being tolerated (**2**−**8**). The substrates with various functional groups, such as ether (**9**), esters (**10**−**12**), amide (**13**), dimethyl malonate (**14**), chlorine (**15** and **16**), and sulfonyl (**17**) groups, also proceeded well without an apparent change in the yield. This was also true for the alkenyl substituents but gave a somewhat decreased yield (**18** and **19**). In addition, the di-iodination product **20** was successfully prepared in 50% yield by using a substrate bearing the OTs group. This was also true for the substrates bearing aryl groups, providing the products **21**−**24** in 42−69% yield.

To further gain insight into the reaction mechanism, we performed density functional theory (DFT) and time-dependent DFT (TDDFT) calculations (see Supporting Information (SI) section 5 for computational details), using truncated NHC and alkenoxypyridinium (namely, **NHC** and **1a**$^+$, respectively).[19] According to the computational results, Figure 1A illustrates our proposed catalytic cycle. On the ground state (S0), **1a**$^+$, NaI, and **NHC** first form a ternary EDA complex **gIM**. Note that the bond distances of Na−I (3.08 Å) and (**NHC**)C−Na (2.48 Å) in **gIM** are close to those (3.03 and 2.50 Å, respectively) in the crystal structure of the NHC−NaI−THF system (Scheme 1B). The N−O bond cleavage in **gIM** requires a barrier of 34.7 kcal/mol (Figure S1 in the SI section 5). The high barrier rationalizes why the reaction could not take place in the absence of blue light irradiation (*supra infra*).

Scheme 3. Scope of the Reaction[a]

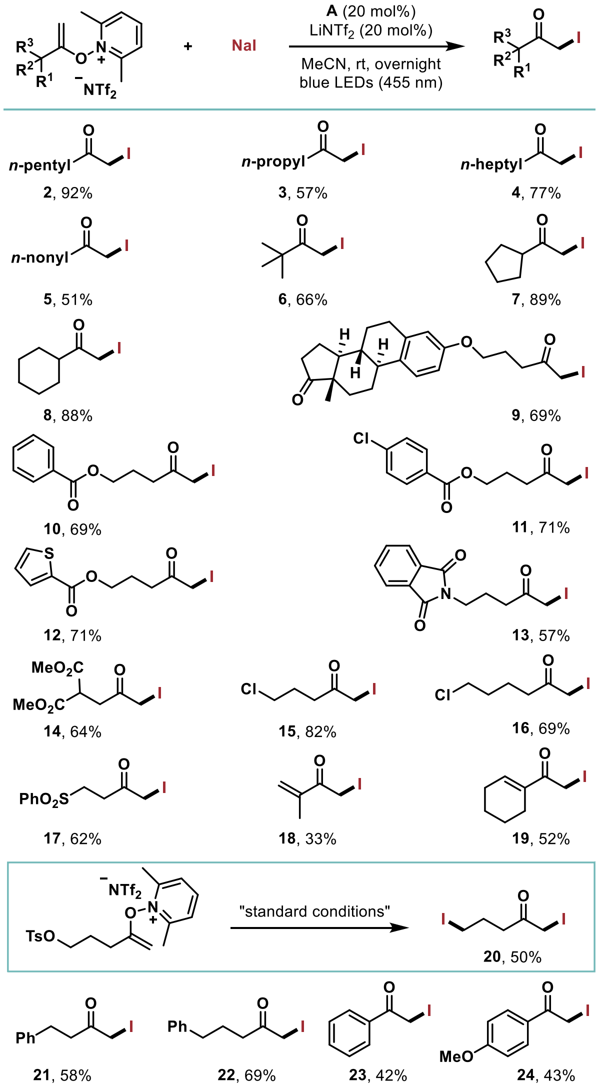

[a]Yield of isolated products **2**–**24** after chromatography.

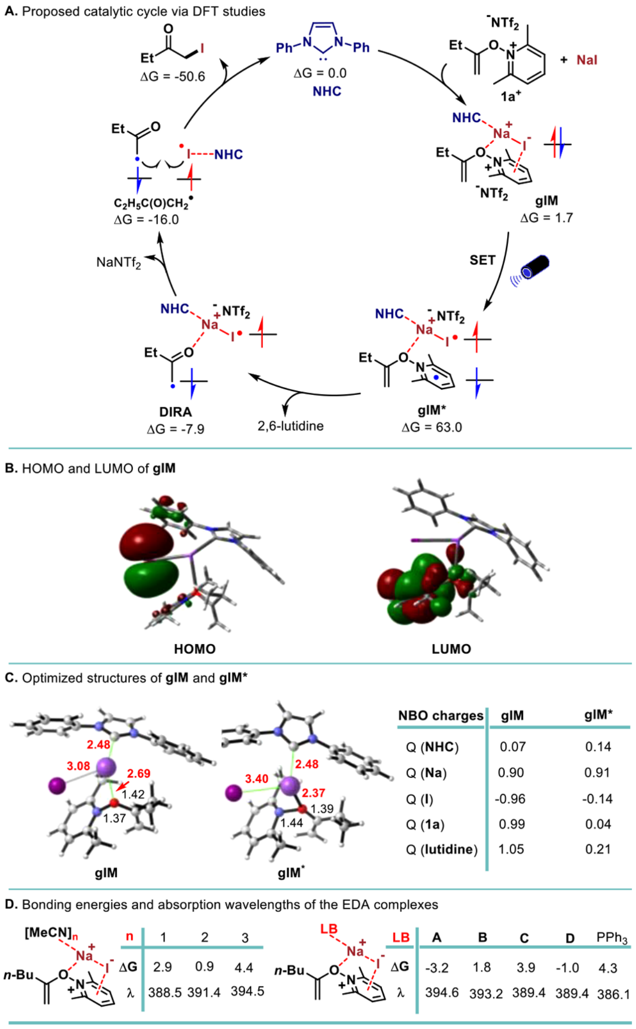

Figure 1. Computational results (**A**–**D**). Key bond lengths in **C** are given in angstroms and NBO charges in *e*. Binding energies in **D** are given in kcal/mol, and absorption wavelengths, in nm.

The HOMO and LUMO of **gIM** are dominated by an iodine lone pair and a π^* orbital of **1a**$^+$, respectively (Figure 1B). The LUMO features somewhat antibonding character on the N–O bond, thus a transition of an electron to LUMO would favor the cleavage of the bond to generate radicals. TDDFT calculation indicated that the vertical excitation of an electron from HOMO to LUMO results in the first excited state (S1) costs 72.6 kcal/mol (394.4 nm). Relaxing the structure of **gIM** in the S1 state gave the photoactivated EDA complex **gIM***. The next process is to cleave the N–O bond in **gIM***, which presumably proceeds via a transition state but attempts to locate the transition state in the S1 state were unsuccessful. Nevertheless, a potential energy surface (PES) scan with the N–O bond as the reaction coordinate demonstrates that **gIM*** is only a very shallow minimum in the S1 state (Table S1 in SI section 5). Thus, under light irradiation, the N–O bond can be broken facilely, leading to a weakly bonded diradical (**DIRA**) and releasing lutidine. Subsequently, the diradical dissociates, giving the $\mathbf{C_2H_5C(O)CH_2^\bullet}$ radical and a radical ion **NHC**-NaI$^{\bullet+}$ which then interacts with NTf$_2^-$ to give an NHC-stabilized iodine radical (**NHC-I$^\bullet$**) via 2c–3e bonding and NaNTf$_2$. Finally, the resultant two radicals combine, affording the α-iodo ketone product.

Although **gIM*** is only a shallow minima in the S1 state, the location of the excited EDA complex facilitates the characterization of the photoactivation process. When the NBO charge populations of **gIM** and **gIM*** are compared in Figure 1C, the excitation increases the charge on iodine from −0.96 to −0.14*e*, while it decreases the total charge on the lutidine fragment from 0.99 to 0.04*e*. The charge variations indicate that the photoactivation promotes SET from iodide to the lutidine moiety of **1a**$^+$. Compared to **gIM**, because the electron redistribution weakens the Coulomb attraction between Na$^+$ and I$^-$ and the Coulomb repulsion between Na$^+$ and the **1a**$^+$ moiety, the Na–I bond is elongated from 3.08 to 3.40 Å and the Na–O bond is shortened from 2.69 to 2.37 Å. In line with our expectation (*supra infra*), the N–O bond is indeed elongated from 1.37 to 1.44 Å, which favors the cleavage of the bond. The charges on **NHC** and the carbenic carbon remain nearly unchanged, indicating no significant electron donation between them.

It is interesting that NHC **A** significantly outperforms other Lewis bases. After understanding the model system, we next considered real systems. Individual reactants (NaI, NHC **A-D**,

https://dx.doi.org/10.1021/acs.orglett.0c02523
Org. Lett. XXXX, XXX, XXX–XXX

PPh_3, and **1**) are all inactive to blue light with absorption wavelengths (<300 nm), but the EDA complexes shown in Figure 1C have significantly increased the absorption wavelength (>380.0 nm). The calculated wavelengths are in reasonable agreement with the wavelength (455 nm) of the blue light we used, considering the accuracy of the TDDFT method which we estimated probably to have an error bar of 50 nm.[20] In addition, the increased wavelengths are consistent with the observed red shift shown in Scheme 2C. As compared in Figure 1D, the Lewis bases only affect the wavelengths slightly but the stabilities of the EDA complexes substantially. In the absence of an NHC, coordination of two acetonitrile solvent molecules to sodium is optimal for the formation of the complexes. In the presence of an NHC, the complex with NHC **A** is more stable than others with NHCs **B**−**D**, which could be a reason for the inferiority of these NHCs.

Compared to NHC **A**, PPh_3 forms a less stable EDA complex (ΔG = 4.3 versus −3.2 kcal/mol of NHC **A**). Figure 2 compares the structures of the EDA complexes of NHC **A** and PPh_3. In the former, NHC **A** forms an "umbrella" to optimally interact with Na^+ via electrostatic interaction, which is not the case for the EDA complexes of PPh_3, as well as those of NHC **B**−**D**, emphasizing the importance of the geometrical uniqueness of NHC **A**. We further compared the binding energies of NHC **A** and PPh_3 with NaI. The large binding energy (−5.3 kcal/mol) of NHC **A** validates the stabilization effect of NHCs on NaI salt via electrostatic interaction. PPh_3 even has a positive binding energy (1.5 kcal/mol) with NaI. In addition, NHC **A** is stronger than PPh_3 in stabilizing the iodine radical (PPh_3 + **A**−I → PPh_3−I + **A** + 4.1 kcal/mol). These advantages of NHC **A** over PPh_3 could be the causes why NHC **A** outperforms PPh_3 in our reaction.

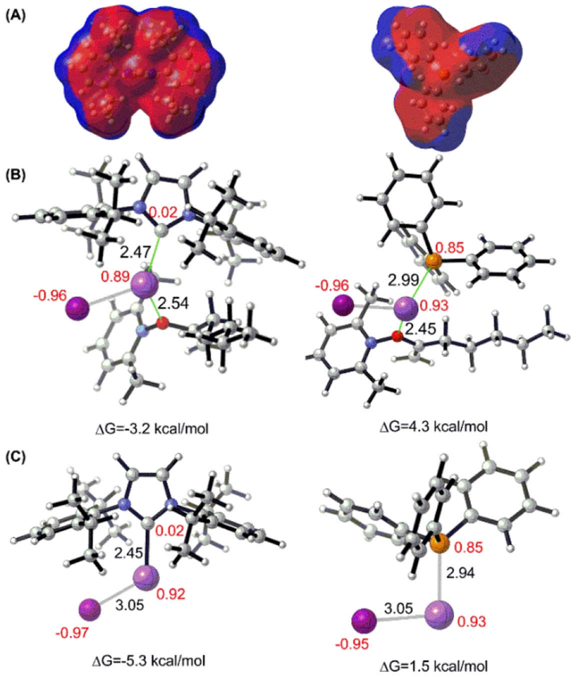

Figure 2. (A) Electrostatic potential maps of NHC **A** (left) and PPh_3 (right). Red areas represent negative electrostatic potential to attract underneath positive Na^+. (B) EDA complexes of NHC **A** and PPh_3 with NaI. (C) Complexes of NHC **A** and PPh_3 with NaI. In (B) and (C), key bond lengths in black are given in angstroms and the NBO charges in red are given in *e*. Binding energies (ΔG) are relative to their separate components.

In summary, we have developed a photocatalytic cross-coupling of *N*-alkenoxypyridinium salts and sodium iodide to afford various α-iodo ketones. Our DFT studies characterize that the electrostatic interaction of NHC−Na^+ facilitates the formation of the EDA complex. In addition, NHC also stabilizes the generated iodine radical via 2c−3e bonding. We anticipate that the presented synthetic method could be applied in the pharmaceutical and organic chemistry arenas. The unveiling of the method of NHC in stabilizing EDA complexes and the mechanistic understanding of the photoactivation process could enrich the photochemistry of EDA complexes and inspire the new development of visible light-induced radical reactions.

■ ASSOCIATED CONTENT

SI Supporting Information

The Supporting Information is available free of charge at https://pubs.acs.org/doi/10.1021/acs.orglett.0c02523.

Experimental details, DFT calculations, characterization data, and spectra (PDF)

■ AUTHOR INFORMATION

Corresponding Authors

Zhi-Xiang Wang − *School of Chemical Sciences, University of the Chinese Academy of Sciences, Beijing 100049, China;* orcid.org/0000-0001-5815-3032; Email: zxwang@ucas.ac.cn

Xiang-Yu Chen − *School of Chemical Sciences, University of the Chinese Academy of Sciences, Beijing 100049, China;* orcid.org/0000-0002-0383-0910; Email: chenxiangyu20@ucas.ac.cn

Authors

He Sheng − *School of Chemical Sciences, University of the Chinese Academy of Sciences, Beijing 100049, China*
Qiang Liu − *School of Chemical Sciences, University of the Chinese Academy of Sciences, Beijing 100049, China*
Xiao-Di Su − *School of Chemical Sciences, University of the Chinese Academy of Sciences, Beijing 100049, China*
Yu Lu − *School of Chemical Sciences, University of the Chinese Academy of Sciences, Beijing 100049, China*

Complete contact information is available at: https://pubs.acs.org/10.1021/acs.orglett.0c02523

Notes

The authors declare no competing financial interest.

■ ACKNOWLEDGMENTS

This paper is dedicated to the memory of Prof. Dieter Enders. Supported by the University of the Chinese Academy of Sciences, National Natural Science Foundation of China (No. 21773240).

■ REFERENCES

(1) (a) Enders, D.; Niemeier, O.; Henseler, A. Organocatalysis by N-Heterocyclic Carbenes. *Chem. Rev.* **2007**, *107*, 5606−5655. (b) Bode, J. W. Carbene Catalysis: An Internal Affair. *Nat. Chem.* **2013**, *5*, 813−815. (c) Hopkinson, M. N.; Richter, C.; Schedler, M.; Glorius, F. An Overview of N-Heterocyclic Carbenes. *Nature* **2014**, *510*, 485−496.

(d) Flanigan, D. M.; Romanov-Michailidis, F.; White, N. A.; Rovis, T. Organocatalytic Reactions Enabled by N-Heterocyclic Carbenes. *Chem. Rev.* **2015**, *115*, 9307−9387. (e) Reyes, E.; Uria, U.; Carrillo, L.; Vicario, J. L. Enantioselective Cascade Reactions under N-Heterocyclic Carbene Catalysis. *Synthesis* **2017**, *49*, 451−471. (f) Zhang, C.; Hooper, J. F.; Lupton, D. W. N-Heterocyclic Carbene Catalysis via the α,β-Unsaturated Acyl Azolium. *ACS Catal.* **2017**, *7*, 2583−2596. (g) Murauski, K. J. R.; Jaworski, A. A.; Scheidt, K. A. A continuing challenge: N-heterocyclic carbene-catalyzed syntheses of γ-butyrolactones. *Chem. Soc. Rev.* **2018**, *47*, 1773−1782. (h) Chen, X.-Y.; Liu, Q.; Chauhan, P.; Enders, D. N-Heterocyclic Carbene Catalysis via Azolium Dienolates: An Efficient Strategy for Remote Enantioselective Functionalizations. *Angew. Chem., Int. Ed.* **2018**, *57*, 3862−3873. (i) Mondal, S.; Yetra, S. R.; Mukherjee, S.; Biju, A. T. NHC-Catalyzed Generation of α,β-Unsaturated Acylazoliums for the Enantioselective Synthesis of Heterocycles and Carbocycles. *Acc. Chem. Res.* **2019**, *52*, 425−436. (j) Chen, X.-Y.; Gao, Z.-H.; Ye, S. Bifunctional N-Heterocyclic Carbenes Derived from l-Pyroglutamic Acid and Their Applications in Enantioselective Organocatalysis. *Acc. Chem. Res.* **2020**, *53*, 690−702.

(2) (a) Guin, J.; De Sarkar, S.; Grimme, S.; Studer, A. Biomimetic Carbene-Catalyzed Oxidations of Aldehydes Using TEMPO. *Angew. Chem., Int. Ed.* **2008**, *47*, 8727−8730. (b) Du, Y.; Wang, Y.; Li, X.; Shao, Y.; Li, G.; Webster, R. D.; Chi, Y. R. N-Heterocyclic Carbene Organocatalytic Reductive β,β-Coupling Reactions of Nitroalkenes via Radical Intermediates. *Org. Lett.* **2014**, *16*, 5678−5681. (c) White, N. A.; Rovis, T. Enantioselective N-Heterocyclic Carbene-Catalyzed β-Hydroxylation of Enals Using Nitroarenes: An Atom Transfer Reaction That Proceeds via Single Electron Transfer. *J. Am. Chem. Soc.* **2014**, *136*, 14674−14677. (d) White, N. A.; Rovis, T. Oxidatively Initiated NHC-Catalyzed Enantioselective Synthesis of 3,4-Disubstituted Cyclopentanones from Enals. *J. Am. Chem. Soc.* **2015**, *137*, 10112−10115. (e) Zhang, Y.; Du, Y.; Huang, Z.; Xu, J.; Wu, X.; Wang, Y.; Wang, M.; Yang, S.; Webster, R. D.; Chi, Y. R. N-Heterocyclic Carbene-Catalyzed Radical Reactions for Highly Enantioselective β-Hydroxylation of Enals. *J. Am. Chem. Soc.* **2015**, *137*, 2416−2419. (f) Chen, X.-Y.; Chen, K.-Q.; Sun, D.-Q.; Ye, S. N-Heterocyclic carbene-catalyzed oxidative [3 + 2] annulation of dioxindoles and enals: cross coupling of homoenolate and enolate. *Chem. Sci.* **2017**, *8*, 1936−1941. (g) Wu, X.; Zhang, Y.; Wang, Y.; Ke, J.; Jeret, M.; Reddi, R. N.; Yang, S.; Song, B.-A.; Chi, Y. R. Polyhalides as Efficient and Mild Oxidants for Oxidative Carbene Organocatalysis by Radical Processes. *Angew. Chem., Int. Ed.* **2017**, *56*, 2942−2946. (h) Zhao, K.; Enders, D. Merging N-Heterocyclic Carbene Catalysis and Single Electron Transfer: A New Strategy for Asymmetric Transformations. *Angew. Chem., Int. Ed.* **2017**, *56*, 3754−3756. (i) Ishii, T.; Ota, K.; Nagao, K.; Ohmiya, H. N-Heterocyclic Carbene-Catalyzed Radical Relay Enabling Vicinal Alkylacylation of Alkenes. *J. Am. Chem. Soc.* **2019**, *141*, 14073−14077. (j) Ishii, T.; Kakeno, Y.; Nagao, K.; Ohmiya, H. N-Heterocyclic Carbene-Catalyzed Decarboxylative Alkylation of Aldehydes. *J. Am. Chem. Soc.* **2019**, *141*, 3854−3858. (k) Song, R.; Chi, Y. R. N-Heterocyclic Carbene Catalyzed Radical Coupling of Aldehydes with Redox-Active Esters. *Angew. Chem., Int. Ed.* **2019**, *58*, 8628−8630. (l) Regnier, V.; Romero, E. A.; Molton, F.; Jazzar, R.; Bertrand, G.; Martin, D. What Are the Radical Intermediates in Oxidative N-Heterocyclic Carbene Organocatalysis? *J. Am. Chem. Soc.* **2019**, *141*, 1109−1117. (m) Kim, I.; Im, H.; Lee, H.; Hong, S. N-Heterocyclic carbene-catalyzed deaminative cross-coupling of aldehydes with Katritzky pyridinium salts. *Chem. Sci.* **2020**, *11*, 3192−3197. (n) Ohmiya, H.; Kakeno, Y. N-Heterocyclic Carbene-Based Catalysis Enabling Cross-Coupling Reactions. *ACS Catal.* **2020**, *10*, 6862−6869. (o) Kakeno, Y.; Kusakabe, M.; Nagao, K.; Ohmiya, H. Direct Synthesis of Dialkyl Ketones from Aliphatic Aldehydes through Radical N-Heterocyclic Carbene Catalysis. *ACS Catal.* **2020**, *10*, 8524−8529. (p) Chen, K.-Q.; Sheng, H.; Liu, Q.; Shao, P.-L.; Chen, X.-Y. N-Heterocyclic Carbene-Catalyzed Radical Reactions. *Sci. China: Chem.* **2020**.

(3) (a) Yoon, T. P.; Ischay, M. A.; Du, J. Visible light photocatalysis as a greener approach to photochemical synthesis. *Nat. Chem.* **2010**, *2*, 527−532. (b) Narayanam, J. M. R.; Stephenson, C. R. J. Visible light photoredox catalysis: applications in organic synthesis. *Chem. Soc. Rev.* **2011**, *40*, 102−113. (c) Prier, C. K.; Rankic, D. A.; MacMillan, D. W. C. Visible Light Photoredox Catalysis with Transition Metal Complexes: Applications in Organic Synthesis. *Chem. Rev.* **2013**, *113*, 5322−5363. (d) Twilton, J.; Le, C.; Zhang, P.; Shaw, M. H.; Evans, R. W.; MacMillan, D. W. C. The merger of transition metal and photocatalysis. *Nat. Rev. Chem.* **2017**, *1*, 0052. (e) Brenninger, C.; Jolliffe, J. D.; Bach, T. Chromophore Activation of α,β-Unsaturated Carbonyl Compounds and Its Application to Enantioselective Photochemical Reactions. *Angew. Chem., Int. Ed.* **2018**, *57*, 14338−14349. (f) Silvi, M.; Melchiorre, P. Enhancing the potential of enantioselective organocatalysis with light. *Nature* **2018**, *554*, 41−49. (g) Zou, Y.-Q.; Hörmann, F. M.; Bach, T. Iminium and enamine catalysis in enantioselective photochemical reactions. *Chem. Soc. Rev.* **2018**, *47*, 278−290. (h) Chen, Y.; Lu, L.-Q.; Yu, D.-G.; Zhu, C.-J.; Xiao, W.-J. Visible light-driven organic photochemical synthesis in China. *Sci. China: Chem.* **2019**, *62*, 24−57. (i) Kancherla, R.; Muralirajan, K.; Sagadevan, A.; Rueping, M. Visible Light-Induced Excited-State Transition-Metal Catalysis. *Trends Chem.* **2019**, *1*, 510−523. (j) McAtee, R. C.; McClain, E. J.; Stephenson, C. R. J. Illuminating Photoredox Catalysis. *Trends Chem.* **2019**, *1*, 111−125. (k) Wei, Y.; Zhou, Q.-Q.; Tan, F.; Lu, L.-Q.; Xiao, W.-J. Visible-Light-Driven Organic Photochemical Reactions in the Absence of External Photocatalysts. *Synthesis* **2019**, *51*, 3021−3054. (l) Zhou, Q.-Q.; Zou, Y.-Q.; Lu, L.-Q.; Xiao, W.-J. Visible-Light-Induced Organic Photochemical Reactions through Energy-Transfer Pathways. *Angew. Chem., Int. Ed.* **2019**, *58*, 1586−1604.

(4) DiRocco, D. A.; Rovis, T. Catalytic Asymmetric α-Acylation of Tertiary Amines Mediated by a Dual Catalysis Mode: N-Heterocyclic Carbene and Photoredox Catalysis. *J. Am. Chem. Soc.* **2012**, *134*, 8094−8097.

(5) Yang, W.; Hu, W.; Dong, X.; Li, X.; Sun, J. N-Heterocyclic Carbene Catalyzed γ-Dihalomethylenation of Enals by Single-Electron Transfer. *Angew. Chem., Int. Ed.* **2016**, *55*, 15783−15786.

(6) (a) Dai, L.; Xia, Z.-H.; Gao, Y.-Y.; Gao, Z.-H.; Ye, S. Visible-Light-Driven N-Heterocyclic Carbene Catalyzed γ- and ϵ-Alkylation with Alkyl Radicals. *Angew. Chem., Int. Ed.* **2019**, *58*, 18124−18130. (b) Gao, Z.-H.; Xia, Z.-H.; Dai, L.; Ye, S. N-Heterocyclic Carbene Catalyzed Photooxidation: Intramolecular Cross Dehydrogenative Coupling of Tetrahydroisoquinoline-Tethered Aldehydes. *Adv. Synth. Catal.* **2020**, *362*, 1819−1824. (c) Xia, Z.-H.; Dai, L.; Gao, Z.-H.; Ye, S. N-Heterocyclic carbene/photo-cocatalyzed oxidative Smiles rearrangement: synthesis of aryl salicylates from O-aryl salicylaldehydes. *Chem. Commun.* **2020**, *56*, 1525−1528. (d) Dai, L.; Ye, S. Photo/N-Heterocyclic Carbene Co-catalyzed Ring Opening and γ-Alkylation of Cyclopropane Enal. *Org. Lett.* **2020**, *22*, 986−990.

(7) Mavroskoufis, A.; Rajes, K.; Golz, P.; Agrawal, A.; Ruß, V.; Götze, J. P.; Hopkinson, M. N. N-Heterocyclic Carbene Catalyzed Photoenolization/Diels−Alder Reaction of Acid Fluorides. *Angew. Chem., Int. Ed.* **2020**, *59*, 3190−3194.

(8) Davies, A. V.; Fitzpatrick, K. P.; Betori, R. C.; Scheidt, K. A. Combined Photoredox and Carbene Catalysis for the Synthesis of Ketones from Carboxylic Acids. *Angew. Chem., Int. Ed.* **2020**, *59*, 9143−9148.

(9) Meng, Q.-Y.; Döben, N.; Studer, A. Cooperative NHC and Photoredox Catalysis for the Synthesis of β-Trifluoromethylated Alkyl Aryl Ketones. *Angew. Chem., Int. Ed.* **2020**, DOI: 10.1002/anie.202008040.

(10) (a) Liu, Q.; Chen, X.-Y. Dual N-heterocyclic carbene/photocatalysis: a new strategy for radical processes. *Org. Chem. Front.* **2020**, *7*, 2082−2087. (b) Mavroskoufis, A.; Jakob, M.; Hopkinson, M. N. Light-Promoted Organocatalysis with N-Heterocyclic Carbenes. *ChemPhotoChem.* **2020**, DOI: 10.1002/cptc.202000120. (c) Liu, J.; Xing, X.-N.; Huang, J.-H.; Lu, L.-Q.; Xiao, W.-J. Light Opens a New Window for N-Heterocyclic Carbene Catalysis. *Chem. Sci.* **2020**, DOI: 10.1039/D0SC03595E.

(11) (a) Poonia, N. S.; Bajaj, A. V. Coordination chemistry of alkali and alkaline earth cations. *Chem. Rev.* **1979**, *79*, 389−445.

(b) Savelyev, A.; Papoian, G. A. Electrostatic, Steric, and Hydration Interactions Favor Na+ Condensation around DNA Compared with K+. *J. Am. Chem. Soc.* **2006**, *128*, 14506−14518. (c) Daniele, P. G.; Foti, C.; Gianguzza, A.; Prenesti, E.; Sammartano, S. Weak alkali and alkaline earth metal complexes of low molecular weight ligands in aqueous solution. *Coord. Chem. Rev.* **2008**, *252*, 1093−1107.

(12) Koch, A.; Görls, H.; Krieck, S.; Westerhausen, M. Coordination behavior of bidentate bis(carbenes) at alkali metal bis(trimethylsilyl)-amides. *Dalton. Trans.* **2017**, *46*, 9058−9067.

(13) (a) Lima, C. G. S.; de M. Lima, T.; Duarte, M.; Jurberg, I. D.; Paixão, M. W. Organic Synthesis Enabled by Light-Irradiation of EDA Complexes: Theoretical Background and Synthetic Applications. *ACS Catal.* **2016**, *6*, 1389−1407. (b) Postigo, A. Electron Donor-Acceptor Complexes in Perfluoroalkylation Reactions. *Eur. J. Org. Chem.* **2018**, *2018*, 6391−6404. (c) Arceo, E.; Jurberg, I. D.; Álvarez-Fernández, A.; Melchiorre, P. Photochemical activity of a key donor−acceptor complex can drive stereoselective catalytic α-alkylation of aldehydes. *Nat. Chem.* **2013**, *5*, 750−756. (d) Crisenza, G. E. M.; Mazzarella, D.; Melchiorre, P. Synthetic Methods Driven by the Photoactivity of Electron Donor−Acceptor Complexes. *J. Am. Chem. Soc.* **2020**, *142*, 5461−5476.

(14) Martin, C. D.; Soleilhavoup, M.; Bertrand, G. Carbene-stabilized main group radicals and radical ions. *Chem. Sci.* **2013**, *4*, 3020−3030.

(15) (a) Seevers, R. H.; Counsell, R. E. Radioiodination techniques for small organic molecules. *Chem. Rev.* **1982**, *82*, 575−590. (b) Stavber, S.; Jereb, M.; Zupan, M. Electrophilic Iodination of Organic Compounds Using Elemental Iodine or Iodides. *Synthesis* **2008**, *2008*, 1487−1513. (c) Podgoršek, A.; Zupan, M.; Iskra, J. Oxidative Halogenation with "Green" Oxidants: Oxygen and Hydrogen Peroxide. *Angew. Chem., Int. Ed.* **2009**, *48*, 8424−8450. (d) Parvatkar, P. T.; Parameswaran, P. S.; Tilve, S. G. Recent Developments in the Synthesis of Five- and Six-Membered Heterocycles Using Molecular Iodine. *Chem. - Eur. J.* **2012**, *18*, 5460−5489. (e) Petrone, D. A.; Ye, J.; Lautens, M. Modern Transition-Metal-Catalyzed Carbon−Halogen Bond Formation. *Chem. Rev.* **2016**, *116*, 8003−8104. (f) Vekariya, R. H.; Balar, C. R.; Sharma, V. S.; Prajapati, N. P.; Vekariya, M. K.; Sharma, A. S. Preparation of α-Iodocarbonyl Compounds: An Overall Development. *ChemistrySelect* **2018**, *3*, 9189−9203.

(16) (a) Li, L.; Liu, W.; Zeng, H.; Mu, X.; Cosa, G.; Mi, Z.; Li, C.-J. Photo-induced Metal-Catalyst-Free Aromatic Finkelstein Reaction. *J. Am. Chem. Soc.* **2015**, *137*, 8328−8331. (b) Liu, W.; Yang, X.; Gao, Y.; Li, C.-J. Simple and Efficient Generation of Aryl Radicals from Aryl Triflates: Synthesis of Aryl Boronates and Aryl Iodides at Room Temperature. *J. Am. Chem. Soc.* **2017**, *139*, 8621−8627.

(17) (a) Fu, M.-C.; Shang, R.; Zhao, B.; Wang, B.; Fu, Y. Photocatalytic decarboxylative alkylations mediated by triphenylphosphine and sodium iodide. *Science* **2019**, *363*, 1429−1434. (b) Noble, A.; Aggarwal, V. K. Triphenylphosphine and sodium iodide: a new catalyst combination to rival precious metal complexes in visible light photoredox catalysis. *Sci. China: Chem.* **2019**, *62*, 1083−1084.

(18) (a) Xu, Z.; Chen, H.; Wang, Z.; Ying, A.; Zhang, L. One-Pot Synthesis of Benzene-Fused Medium-Ring Ketones: Gold Catalysis-Enabled Enolate Umpolung Reactivity. *J. Am. Chem. Soc.* **2016**, *138*, 5515−5518. (b) Xu, Z.; Zhai, R.; Liang, T.; Zhang, L. Efficient One-Pot Multifunctionalization of Alkynes en Route to α-Alkoxyketones, α-Thioketones, and α-Thio Thioketals by using an Umpolung Strategy. *Chem. - Eur. J.* **2017**, *23*, 14133−14137. (c) Petrosyan, A.; Hauptmann, R.; Pospech, J. Heteroarene N-Oxides as Oxygen Source in Organic Reactions. *Eur. J. Org. Chem.* **2018**, *2018*, 5237−5252. (d) Xia, X.; Chen, B.; Zeng, X.; Xu, B. Synthesis of α-amino ketones through aminations of umpoled enolates. *Org. Biomol. Chem.* **2018**, *16*, 6918−6922. (e) Xia, X.; Chen, B.; Zeng, X.; Xu, B. Synthesis of α-Trifluoromethylthiolated and α-Thiocyanated Ketones Using Umpoled Enolates. *Adv. Synth. Catal.* **2018**, *360*, 4429−4434. (f) Zhai, R. L.; Xue, Y. S.; Liang, T.; Mi, J. J.; Xu, Z. Regioselective Arene and Heteroarene Functionalization: N-Alkenoxypyridinium Salts as Electrophilic Alkylating Agents for the Synthesis of α-Aryl/α-Heteroaryl Ketones. *J. Org. Chem.* **2018**, *83*, 10051−10059. (g) Mathi, G. R.; Jeong, Y.; Moon, Y.; Hong, S. Photochemical Carbopyridylation of Alkenes Using N-Alkenoxypyridinium Salts as Bifunctional Reagents. *Angew. Chem., Int. Ed.* **2020**, *59*, 2049−2054. (h) Liu, Q.; Zhang, C.-S.; Sheng, H.; Enders, D.; Wang, Z.-X.; Chen, X.-Y. Site-Selective Pyridyl Alkyl Ketone Synthesis from N-Alkenoxypyridiniums through Boekelheide-Type Rearrangements. *Org. Lett.* **2020**, *22*, 5617−5621.

(19) For selected examples of computational investigations of NHC catalysis, see: (a) Zheng, L.; Wang, Y.; Wei, D.; Qiao, Y. Insights into N-Heterocyclic Carbene-Catalyzed [4 + 2] Annulation Reaction of Enals with Nitroalkenes: Mechanisms, Origin of Chemo- and Stereoselectivity, and Role of Catalyst. *Chem. - Asian J.* **2016**, *11*, 3046−3054. (b) Li, X.; Wang, Y.; Wang, Y.; Tang, M.; Qu, L.-B.; Li, Z.; Wei, D. Insights into the N-Heterocyclic Carbene (NHC)-Catalyzed Oxidative γ-C(sp3)−H Deprotonation of Alkylenals and Cascade [4 + 2] Cycloaddition with Alkenylisoxazoles. *J. Org. Chem.* **2018**, *83*, 8543−8555. (c) Wang, Y.; Wei, D.; Zhang, W. Recent Advances on Computational Investigations of N-Heterocyclic Carbene Catalyzed Cycloaddition/Annulation Reactions: Mechanism and Origin of Selectivities. *ChemCatChem* **2018**, *10*, 338−360. (d) Li, X.; Xu, J.; Li, S.-J.; Qu, L.-B.; Li, Z.; Chi, Y. R.; Wei, D.; Lan, Y. Prediction of NHC-catalyzed chemoselective functionalizations of carbonyl compounds: a general mechanistic map. *Chem. Sci.* **2020**, *11*, 7214−7225.

(20) According to Truhlar et al.'s calibrations: Jacquemin, D.; Perpète, E. A.; Ciofini, I.; Adamo, C.; Valero, R.; Zhao, Y.; Truhlar, D. G. Time-Dependent Density Functional Theory "Not Guilty" of Large Errors for Cyanines. *J. Chem. Theory Comput.* **2010**, *6*, 2071−2085. Regarding TDDFT-M06 calculations for a set of 18 n→p* transitions of neutral nitroso dyes, the mean unsigned deviation is 0.39 eV. Taking the value into account, the error bar for a wavelength of 400.0 nm is about 50.0 nm.